ELSEVIER

Experimental Thermal and Fluid Science 19 (1999) 223–232

Experimental Thermal and Fluid Science

www.elsevier.nl/locate/etfs

Entry region of louvered fin heat exchangers

Marlow E. Springer, Karen A. Thole *,[1]

Mechanical Engineering Department, University of Wisconsin, Madison, Wisconsin 53706, USA

Received 9 September 1998; received in revised form 17 June 1999; accepted 1 July 1999

Abstract

The dominant thermal resistance for most compact heat exchangers occurs on the gas side and as such an understanding of the gas side flowfield is needed before improving current designs. Louvered fins are commonly used in many compact heat exchangers to increase the surface area and initiate new boundary layer growth. For this study, detailed flowfield measurements were made in the entry region of several louvered fin geometries whereby the louver angle, ratio of fin pitch to louver pitch, and Reynolds number were all varied. In addition to mean velocity measurements, time-resolved velocity measurements were made to quantify unsteady effects.

The results indicated larger fin pitches resulted in lower average flow angles in the louver passages and longer development lengths. Larger louver angles with a constant ratio of fin pitch to louver pitch resulted in higher average flow angles and shorter development lengths. As the Reynolds number increased, longer development lengths were required and higher average flow angles occurred as compared with a lower Reynolds number case. Time-resolved velocity measurements indicated some flow periodicity behind the fully developed louver for a range of Reynolds numbers. The Strouhal number of these fluctuations was constant for a given louver geometry, but the value increased with increasing fin pitch.

Keywords: Heat exchangers; Louvered fins; Interrupted surfaces

1. Introduction

Louvered fin compact heat exchangers are used extensively in several automotive applications such as radiators, oil coolers, condensers, and charge air coolers. The purpose of placing louvers on the fin is to provide additional heat transfer surface area and to interrupt the growth of the boundary layer forming along the fin surface. This new boundary layer formation provides a high heat transfer region along the fin. Under typical operating conditions of most fin-and-tube air-and-water heat exchangers the dominating thermal resistance is on the air (external) side and can be as much as 95% of the total thermal resistance. By achieving a better understanding of the flows in the louvered fins, methods of reducing the thermal resistance can be developed which will ultimately lead to a reduction in space, weight, and cost of louvered fin heat exchangers.

One region, in particular, that is important for the understanding of the performance of a compact heat exchanger is the air-side entry region. As the flow progresses streamwise through several louver passages, the flow becomes hydrodynamically fully developed. This paper describes the effects of geometry and Reynolds number on the air flow in the entry region of a compact heat exchanger. In addition, there has been some evidence in the literature that periodic shedding from the louvers can occur. This paper also addresses when, if at all, this shedding occurs downstream of the first louver in the fully developed flow region.

2. Past studies

Detailed studies of compact heat exchangers date back to the hot-wire anemometry and flow visualization work performed by Beauvais [1]. Much later Davenport [2,3] performed flow visualization studies and concluded that while hydraulic diameter is relevant to heat transfer in plain fins, the heat transfer for louvered fins is more appropriately described by a Reynolds number based on the louver pitch.

* Corresponding author. Tel.: +1-540-231-7192; fax: +1-540-231-9100; e-mail: thole@vt.edu

[1] Present address: Mechanical Engineering Department, Virginia Polytechnic Institute and State University, Blacksburg, VA 24061, USA.

0894-1777/99/$ - see front matter
PII: S0894-1777(99)00028-X

Antoniou et al. [4] performed detailed two component hot-wire measurements in a scaled-up model of louvered fins for a fairly large ratio of fin pitch to louver pitch of $F_p/L_p = 1.7$ with a louver angle of $\theta = 25°$. Their results indicated an increase in the mean flow angle for each streamwise louver until approximately the fourth louver. Beyond the fourth louver, the mean flow angle maintained a value slightly less than the louver angle, with that value depending on Reynolds number. With Reynolds numbers at and above 1000, they reported high velocity fluctuations and hypothesized that these were caused by vortices being shed from the louvers.

Mochizuki and Yagi [5] also used hot-wire anemometry to record velocity fluctuations and perform spectral analyses of the shedding behind a parallel array of interrupted surfaces. Their data indicated that for a single plate, as the Reynolds number increased to 250 separation moved from the trailing edge to the leading edge. Two shedding frequencies occurred with two columns of offset fins at a Reynolds number of 163, with the upstream stage showing a higher frequency. With multiple stages, they noted a Reynolds number effect on the beginning of shedding. At a Reynolds number of 44, the wake some distance downstream of the bank began to oscillate. As the Reynolds number increased to 53, the shedding moved from the exit louver into the upstream stages in the bank, and transition from laminar to turbulent flow occurred by a Reynolds number of 154. With nine or more fin stages, they measured one shedding frequency with a Strouhal number of 0.13.

Amon et al. [6] performed numerical and experimental studies of flows in parallel communicating channels with periodic in-line plates. They found improved heat transfer due to the periodic interruptions of the heat transfer surface, and also due to the shedding vortices which induced mixing in the flows. They also indicated increased pressure drop associated with the higher skin friction from the periodic restarting of the boundary layer and the creation of the separated flow regions. The flows exhibited a quasi-periodic state composed of the sum of two periodic functions, and the power spectra showed two peaks at the fundamental frequencies. Their results showed vortices were ejected alternately from the top and bottom surfaces of the plates. Numerical predictions by Zhang [7] for an inclined louver also showed unsteady effects. At a Reynolds number of 162, his calculations showed a steady wake region downstream of the trailing edge, with steady flow until the Reynolds number reached 782. Beyond this Reynolds number, the flow became unsteady with vortex shedding from the leading edge of the louver on the back side.

DeJong and Jacobi [8] showed the effects of boundary layer growth and vortex shedding in parallel plate arrays with offset-strip geometries through flow visualization in a water tunnel. At a low Reynolds number of 380, there were steady, laminar recirculating eddies in the wake of each plate in the array. At a Reynolds number of 550, a secondary periodic flow formed at the fourth or fifth louver from the array entrance. This formed a "feathery wake" consisting of secondary vortices stretched by a velocity gradient and advected downstream. By a Reynolds number of 720, there was large scale vortex shedding in the array, with vortex shedding at the leading edges of the plates. As the Reynolds number was increased, the onset of vortex shedding occurred earlier in the plate array. At a Reynolds number of 1060, the first plate was shedding vortices, and the flow had become turbulent by about the sixth plate location. The investigators speculated that vortex shedding first occurred at the trailing edge of the last plate in the array. As the Reynolds number increased, the shedding progressed forward to the earlier plates. Shedding vortices from the trailing edge of a plate allowed vortices to be shed from the leading edge of the downstream plate. This behavior was seen earlier in the array at higher Reynolds numbers.

3. Experimental approach

The louvered fin-and-tube design that was investigated is illustrated in Fig. 1(a). The main focus is on the louvered fin array with the geometrical parameters of interest illustrated in Fig. 1(b). Table 1 summarizes the six different louvered fin geometries that were studied. For all of these studies the louver pitch and length were held constant at 27.9 mm and the louver thickness was also held constant at 2.28 mm.

For the experiments reported in this paper, 20:1 scaled up models were placed in the test apparatus shown in Fig. 2. The CFD results presented by Springer and Thole [9] pointed out the importance of experimentally simulating a large number of louver rows when scaling up the louver models to insure that the flow is not affected by the endwalls. This study showed that by using too few louver rows, the flow was forced to be duct directed by the endwalls as opposed to being louver directed. The number of louver rows in the models that were used for this study ranged between 15 and 20. In addition, the flows being considered for all of the models in Table 1 were all louver directed. A valid measurement regime was identified through CFD studies and was experimentally validated for these different geometries (Springer and Thole [10]). This region, which follows a particle path, is indicated in Fig. 2 with a close-up given in Fig. 3(a). Fig. 3(a) also illustrates the cut locations where velocity measurements were made. This study has focused on the entry region of the scaled up model upstream of the turning louver (cuts 1a–6).

The test apparatus, shown in Fig. 2, included a settling chamber to condition the flow upstream of the test section. At the entrance to the test section, screens and foam were used to straighten the incoming flow and achieve good flow uniformity with reduced turbulence levels. The Styrofoam popcorn was placed in the settling chamber to reduce any fan-induced flow frequencies. The flow uniformity across the louver flow paths upstream of the test section was quantified in terms of a

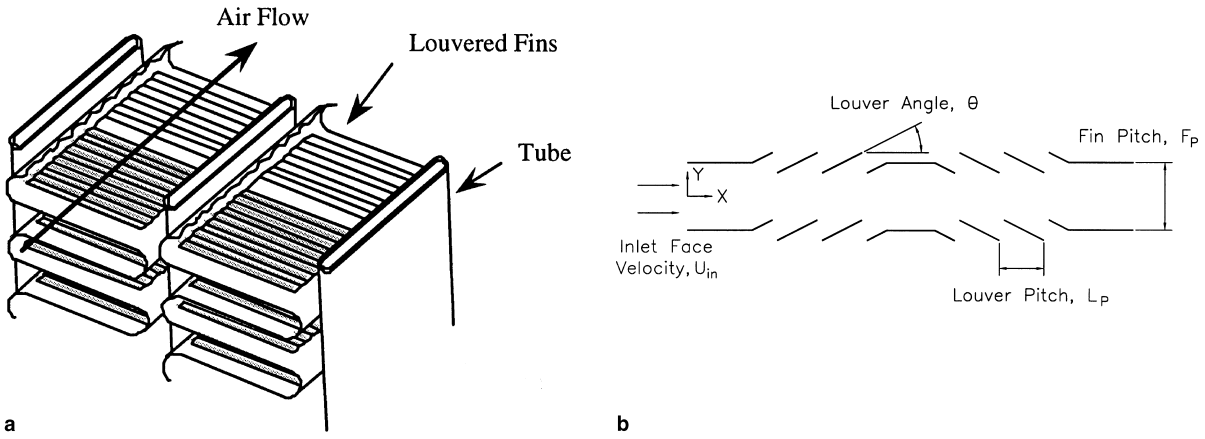

Fig. 1. (a) Schematic of louvered fin-and-tube heat exchanger. (b) Illustration of the geometrical parameters of interest for a louvered fin.

Table 1
Summary of louvered fin geometry

Louver angle	27°	27°	27°	39°	39°	39°
Fin pitch to louver pitch (F_p/L_p)	0.76	0.91	1.52	0.91	1.22	1.52
Fin thickness to louver pitch (t/L_p)	0.08	0.08	0.08	0.08	0.08	0.08
Number of louvers	17	17	17	17	17	17

maximum deviation from the average velocity. The maximum deviation for the $F_p/L_p = 0.76$ and 1.52 were 1.9% and 2.6%, respectively.

A two-component laser Doppler velocimeter (LDV) system was used to measure the mean velocities (u and v) in the louvered fin arrays. These velocities were then used to quantify the flow angle (α) as well as the total velocity (V). An LDV has the advantage of not interrupting the flow, which is particularly important in laminar unsteady flows, but does require optical access. Optical access was possible such that bulk velocities were measured between 65% and 75% of the louver passage flow area. The focal length of the lens was 350 mm with a half-angle of 3.9° giving a probe volume that was 90 μm in diameter and 1.3 mm in length. Incense smoke was used as LDV seed particles, which were generated outside the main loop and injected just upstream of the settling chamber. Mean horizontal (u) and vertical (v) velocity components were obtained by sampling 5000 points taken over a 15–20 s period at each measurement location. The mean velocities were calculated using residence time weighting as the velocity bias correction technique. Time resolved velocity measurements of 30 000 points of the component parallel to the louver angle were obtained during a time of nominally 30 s. An averaging and interpolation routine was developed to create an equal time spaced data set from the unequally spaced raw LDV data. This data was then put into an FFT routine to calculate the energy spectra.

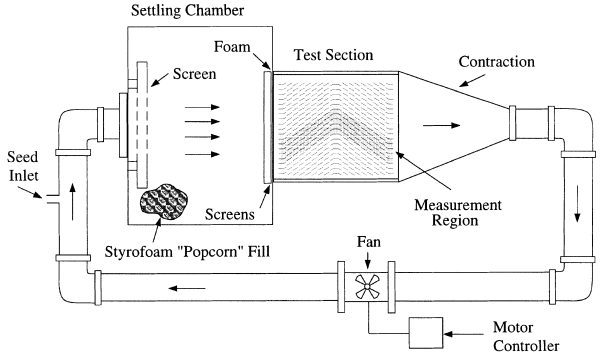

Fig. 2. Experiemental test set-up with 20:1 scaled-up louver models.

4. Experimental uncertainties

Velocity measurements taken several months apart for the same flow conditions at the same given location that indicated very good repeatability (Springer and Thole [10]). Uncertainties in the quantities presented were based on the methods presented by Moffat [11]. The bias uncertainty in the individual velocity component measurements was found to be a maximum of 1.04%, arising from uncertainties in the Doppler frequencies and the fringe spacing of the probe volume beam crossing. Possible misalignment of the horizontal planes of the probe traverse mechanism and the louvered fin test section gave rise to uncertainty in the measured flow angle. This offset in the rotation of the coordinate system for the bulk velocity measurements was estimated to be a maximum of 0.5°. The combined effects of the bias errors inherent in the LDV system and the possible probe volume coordinate system mismatch

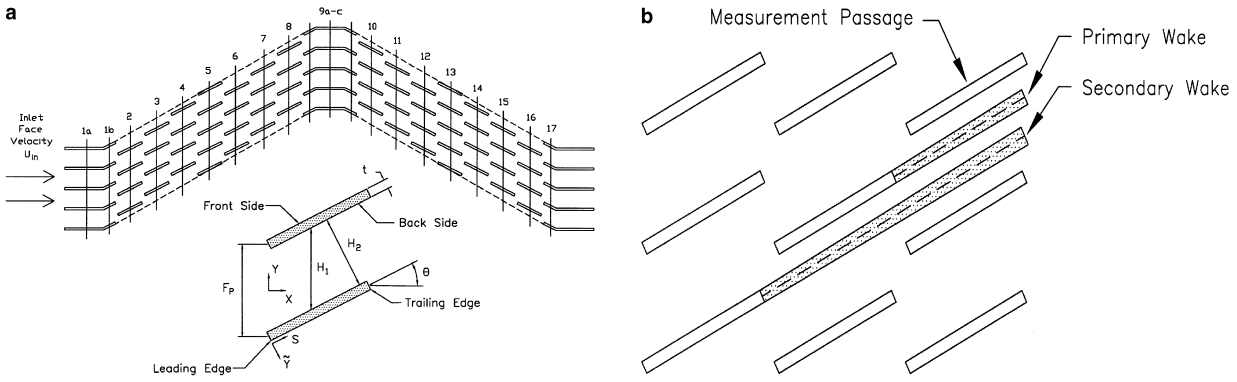

Fig. 3. (a) Locations of measurement cuts for bulk flow in the louver passages. (b) Illustration of the primary and secondary wake terminology.

relative to the test section yielded uncertainties in the total flow angle of 10.1% at a flow angle of 5°, and 1.57% at a flow angle of 45°. Note that beyond the first louver, the flow angle is typically 20° or higher, yielding an uncertainty near 2% for the majority of the bulk flow measurements. The velocity precision error with a 95% confidence interval was a maximum of 0.1%, based on mean velocity measurements, with those cases exhibiting periodic flow instabilities showing slightly larger error but still a maximum of 0.1%.

5. Developing flow region

This section discusses the bulk flowfields through the louver arrays from the inlet deflection louver to the fully developed louver position. Note that these profiles were taken at the streamwise midpoint position along the louver at a cut perpendicular to the axial flow direction. The flowfield results will be characterized through the velocity magnitude and flow angle profiles moving through the louvers for the different geometries and Reynolds numbers. Two different wake regions will be discussed in this section and are referred to as primary and secondary wakes, which are defined by the location of the louver that created the wake with respect to the measurement passage. If the louver creating the wake is immediately upstream of the measurement passage, it is the primary wake. If the wake is created by the louver two positions upstream, then it is referred to as the secondary wake. Fig. 3(b) illustrates the terminology for the primary and secondary wakes. The effect of the ratio of fin pitch to louver pitch and the effect of louver angle will be discussed with regards to the developing flow region.

5.1. Effect of fin pitch to louver pitch

Three different fin pitches were investigated at each of the two different louver angles, as was indicated in Table 1. Recall that the louver pitch remained constant for each of the cases investigated. Figs. 4(a), (b), and 5 (a), (b) show the total velocity magnitude and flow angle profiles for the 27° louver angle at the smallest fin pitch ($F_p/L_p = 0.76$) for both the low and high Reynolds numbers studied. For the case at $Re_{Lp} = 230$, shown in Fig. 4(a) and (b), it is clear that the cut 1a profile exhibits a developing channel type flow with fairly thick boundary layers. Cut 1b shows an asymmetric profile with a higher velocity region nearer to the top of the louver passage where the flow is deflected by the inlet louver. The flow angles show that, within the measurement uncertainty, the flow entering the louver (cut 1a) is straight relative to the inlet louver. The flow is quickly turned as evidenced by the profiles measured at cut 1b, but is still significantly below the louver angle. For this

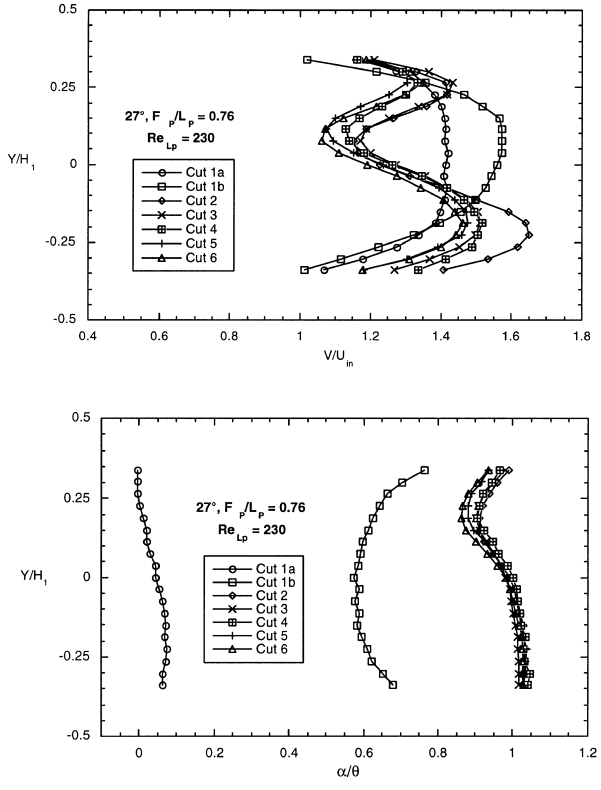

Fig. 4. (a), (b) Velocity magnitude and flow angle profiles showing development through the louver bank for $\theta = 27°$ and $F_p/L_p = 0.76$ at $Re_{Lp} = 230$.

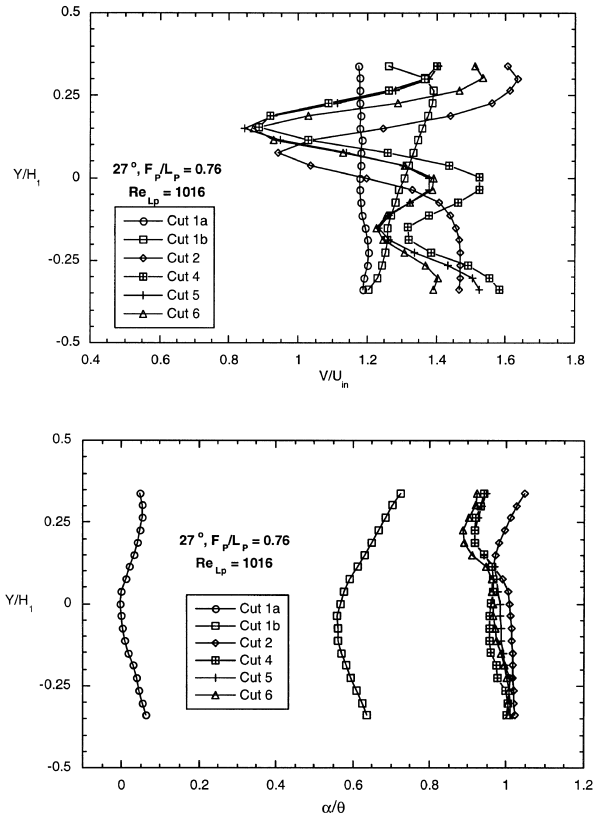

Fig. 5. (a), (b) Velocity magnitude and flow angle profiles showing development through the louver bank for $\theta = 27°$ and $F_p/L_p = 0.76$ at $Re_{Lp} = 1016$.

particular geometry and Reynolds number, cut 2 still showed slight changes in the velocity profile, but cuts 3–6 looked fairly similar. The primary wake appeared for cut 2 at $Y/H_l = 0.13$, with the minimum velocity having a value of 1.15 U_{in}. The average flow angle, which was computed over the region shown in Fig. 4(b), at cut 2 was quite high at 0.98θ. By the third louver the overall shape of the profile was the same as occurred for the downstream louvers. The minimum velocity had not changed much between the third through sixth louver locations dropping to 1.1 U_{in}. With the overall average flow angle slightly less than the louver angle, the flow was directed more towards the lower louver than the upper louver. This caused the front side of the lower louver to affect the flow more like a physical wall than the upper louver; therefore, the flow was more louver directed near the bottom of the passage.

For the same geometry at a higher Reynolds number of $Re_{Lp} = 1016$, Fig. 5(a) and (b) show the velocities in the measurement region were constant for cut 1a indicating that the boundary layer was outside of the measurement region and therefore much thinner. Due to the thinner boundary layer, the relative velocity magnitudes were much slower than the peak velocity for the lower Reynolds number case. At this higher Reynolds number cut 1b showed even more of an asymmetric profile with higher velocities nearer the top of the passage. For cut 2 the primary wake appeared at $Y/H_l = 0.07$. Further downstream, by the third and fourth louver, this wake appeared slightly higher in the passage at $Y/H_l = 0.15$, and the secondary wake also appeared. (Note the profile for cut 3 was omitted for clarity.) This secondary wake was formed from the inlet deflection louver and was not evident for the $Re_{Lp} = 230$ case. The primary wake was lower in the second louver passage due to the low average flow angle exiting the first louver (cut 1b), which was 0.62θ. The flow exiting the second passage and entering the third passage was at a higher angle (1.01θ at cut 2), thus raising the position of the primary wake in the third and subsequent louver passages. The final position of the primary wake was slightly higher in the passage than for the low Reynolds number. Similar to the $Re_{Lp} = 230$ case, the velocity magnitude profiles still showed some changes at cuts 3 and 4, but cuts 5 and 6 were quite similar. In the fourth through sixth louvers the minimum velocity in the primary wake region was about $0.85U_{in}$, lower than for $Re_{Lp} = 230$, indicating a more pronounced deficit effect at the higher Reynolds number. The secondary wake was evident in the third louver passage at $Y/H_l = -0.2$, with a minimum velocity of $1.17U_{in}$. In the fifth and sixth passages, the secondary wake was at $Y/H_l = -0.15$, with a minimum velocity of $1.24U_{in}$. The α/θ behavior was much the same for the two Reynolds number cases, in both magnitude and shape except for cut 2. For $Re_{Lp} = 230$, the characteristic shape of the angle profiles are already similar to the downstream profiles whereas for $Re_{Lp} = 1016$ the shape is somewhat different.

For a wider fin pitch spacing the flowfield in the louvers took longer to develop when comparing the $F_p/L_p = 1.52$ to the $F_p/L_p = 0.76$ case. For the $F_p/L_p = 1.52$ case at $Re_{Lp} = 230$, shown in Fig. 6(a) and (b), the passages beyond the second louver showed effects of the wake from two louvers upstream, unlike the case with $F_p/L_p = 0.76$ at $Re_{Lp} = 230$. Also, the relative positions of the primary and secondary wakes switched, i.e. the primary wake was at the bottom of the louver passage, while it was at the upper portion for the $F_p/L_p = 0.76$ case. There were some slight changes in the velocity profiles when comparing cuts 5 and 6 while the profile for cut 7 was nearly identical to cut 6. The primary wake was located at $Y/H_l = -0.19$ by the fifth and sixth passages. The secondary wake appeared as a slight kink in the third louver passage at $Y/H_l = -0.05$, and moved to $Y/H_l = 0.10$ by the fifth and sixth louvers. The minimum velocity in the primary wake was $0.88U_{in}$ and $0.82U_{in}$ at cuts 5 and 6, lower than for the same Reynolds number case with $F_p/L_p = 0.76$. This showed that the wider fin spacing allowed the wake region from upstream louvers to have a more prolonged effect in the passages. The α/θ profiles indicate that only the fifth and sixth louvers were matched. At cut 1b, the average flow angle was 0.40θ, lower than that with $F_p/L_p = 0.76$. By the fifth and sixth louvers, the mean flow angles were 0.86θ and 0.85θ. These results agree with findings by previous investigators that showed that a larger ratio of fin pitch to louver pitch tended to a

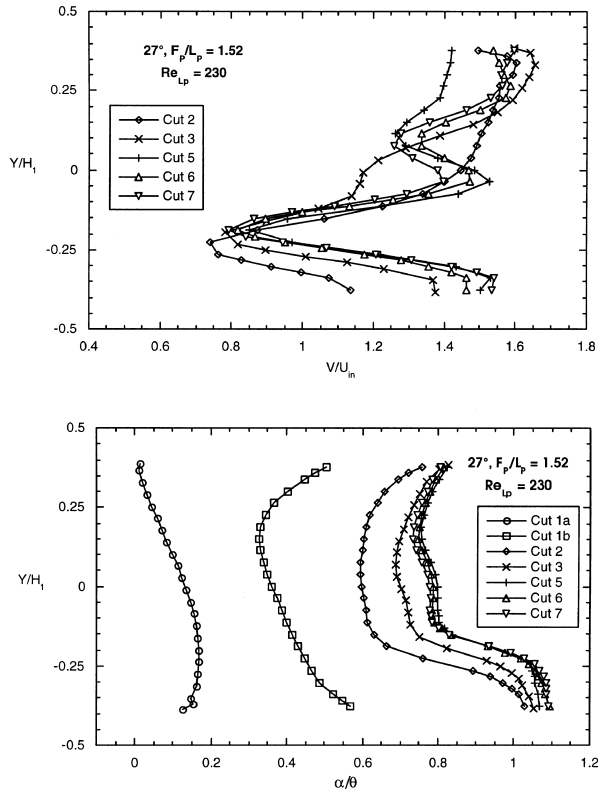

Fig. 6. (a), (b) Velocity magnitude and flow angle profiles showing development through the louver bank for $\theta = 27°$ and $F_p/L_p = 1.52$ at $Re_{Lp} = 230$.

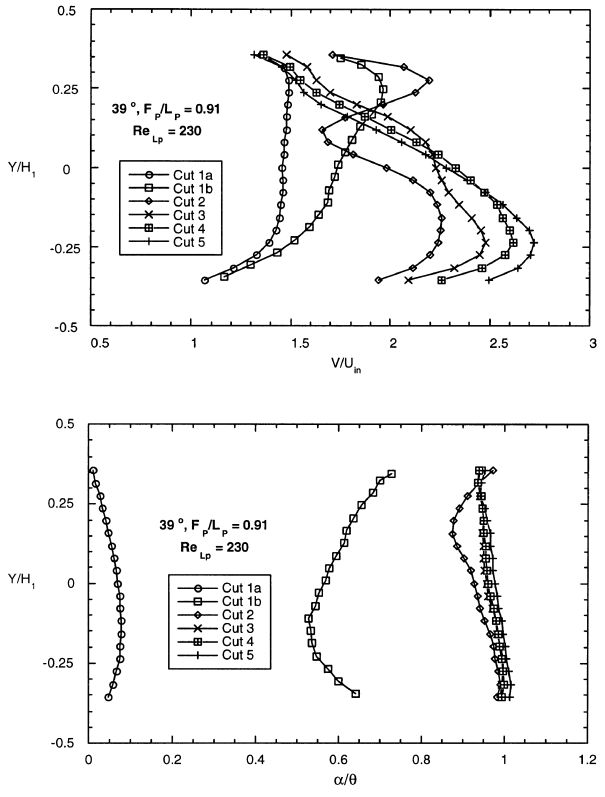

Fig. 7. (a), (b) Velocity magnitude and flow angle profiles showing development through the louver bank for $\theta = 39°$ and $F_p/L_p = 0.91$ at $Re_{Lp} = 230$.

slightly more duct directed flow. Note that the flow angles were again higher closer to the bottom of the louver passage.

The differences between the two ratios of fin pitch to louver pitch at $Re_{Lp} = 230$ indicated that the larger ratio causes the effects of the wakes from the louvers to progress farther through the louver passages, and also that the flow required more louvers to reach the fully-developed condition. This trend was also shown at the higher Reynolds numbers for this geometry ($F_p/L_p = 1.52$). These findings are in disagreement with Antoniou et al. (1990) who found that the flow angle reached a constant value at the fourth louver position for a large fin pitch of $F_p/L_p = 1.7$ at a louver angle of $\theta = 25°$. This disagreement may be due to the fact that Antoniou et al. (1990) only used seven louver rows for their scaled-up model. The results presented by Springer and Thole [10] suggest that a much larger number of louver rows are needed in order to avoid endwall effects.

For a louver angle of 39° at the smallest ratio of fin pitch to louver pitch ($F_p/L_p = 0.91$) studied, Fig. 7(a) and (b) shows the bulk velocity measurements for $Re_{Lp} = 230$. For this geometry, the flow showed some interesting developments at the inlet. A fairly strong wake from the first louver appeared in the second louver passage at $Y/H_1 = 0.11$ for cut 2. As the flow progressed downstream, the velocity deficit from this primary wake was significantly reduced and was barely seen in the remaining passages. Only a small deficit was apparent at $Y/H_1 = 0.28$ in and beyond the third louver passage. In the third louver passage, there was also a small deficit in the profile at $Y/H_1 = -0.07$, which was caused by the louver located two positions upstream. Beyond the fourth louver passage, the profiles showed no significant changes. In the fourth louver passage there was no secondary wake and only the small effect of the louver immediately upstream remained near the top of the passage. The third through sixth louver passages all showed basically a linear decrease in flow angle from the bottom of the passage (also the bottom of the cut) to the top. The average flow angles for both the fifth and sixth louvers were 0.98θ. Note that for the case with $\theta = 27°$, $F_p/L_p = 0.91$, and $Re_{Lp} = 230$, the average flow angle at cut 6 was 0.93θ, which showed that the lower louver angle yielded a lower flow efficiency.

Fig. 8(a) and (b) show profiles for $\theta = 39°$, $F_p/L_p = 1.22$, and $Re_{Lp} = 230$. The primary wake appeared in the second louver passage at $Y/H_1 = -0.08$, then progressed up to $Y/H_1 = 0.11$ farther downstream as the average flow angle increased. Unlike the $F_p/L_p = 0.91$ case, the wake produced by the louver two positions upstream was not evident in the third louver passage, but did appear in cuts 4 and 5. In the fourth and fifth louver passages, this secondary wake was centered at $Y/H_1 = -0.23$. The average flow angles at cuts 4 and 5 were 0.93θ, slightly lower than for the

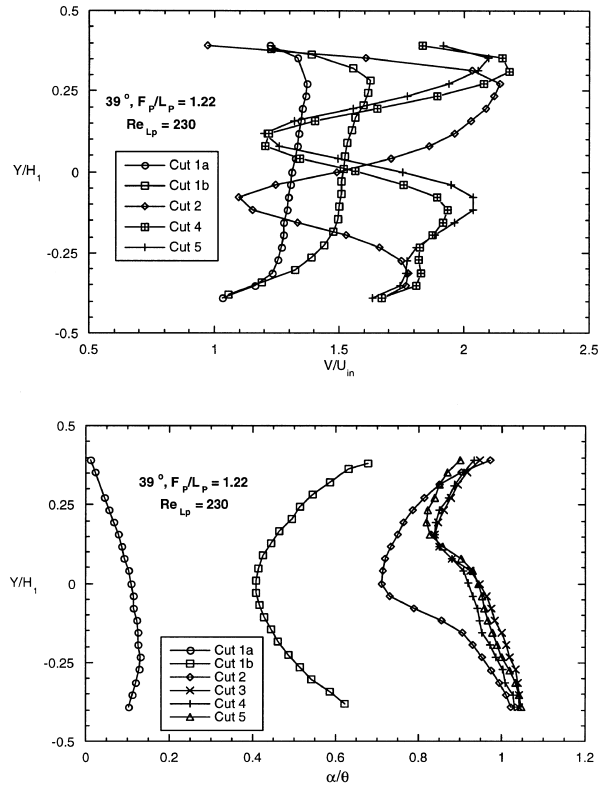

Fig. 8. (a), (b) Velocity magnitude and flow angle profiles showing development through the louver bank for $\theta = 39°$ and $F_p/L_p = 1.22$ at $Re_{Lp} = 230$.

previous geometry. This was to be expected due to the larger ratio of fin pitch to louver pitch.

Based on the results discussed above most of the data indicated that while changes in the velocity magnitude profiles were still occurring as the flow progressed through the louvers, changes in the flow angle profiles indicated fully developed conditions much sooner. As the ratio of fin pitch to louver pitch increased from $F_p/L_p = 0.76$ to 1.52, the number of streamwise louvers needed to reach a velocity profile that remained the same increased from three to five. As the Reynolds number increased, the number of louvers required to reach fully developed conditions also increased.

Fig. 9 shows the mean flow angle normalized by the louver angle for the developing flowfield regions upstream of the central turning louver for several different fin pitches and the two different louver angles at $Re_{Lp} = 230$. From this data, it is clear that the as the ratio of fin pitch to louver pitch increased a longer streamwise distance was required before a constant value occurred. For the $F_p/L_p = 1.52$ cases, the flow angles reached a fairly constant value by the fifth louver. As discussed earlier, the larger fin pitches resulted in lower average flow angles. These results are consistent with the $Re_{Lp} = 1016$ case except that generally higher average flow angles for a given louver position occurred for $Re_{Lp} = 1016$.

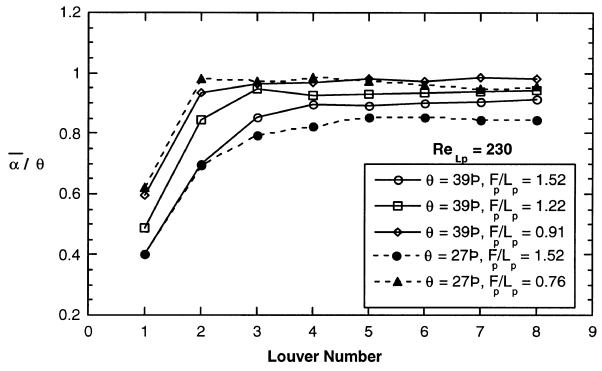

Fig. 9. Effect of fin pitch and louver angle on the average flow angle progressing through the louvers for $Re_{Lp} = 230$.

5.2. Effect of louver angle

Fig. 10(a) and (b) show the velocity magnitude and flow angles for the same ratio of fin pitch to louver pitch as discussed earlier of $F_p/L_p = 1.52$ (Fig. 6(a) and (b)) but for a higher louver angle of $\theta = 39°$. At the louver entrance (cut 1a), the velocities were slightly higher at the top of the passage, but for cut 1b, the velocity profile was much flatter with only a slight defect near the top of

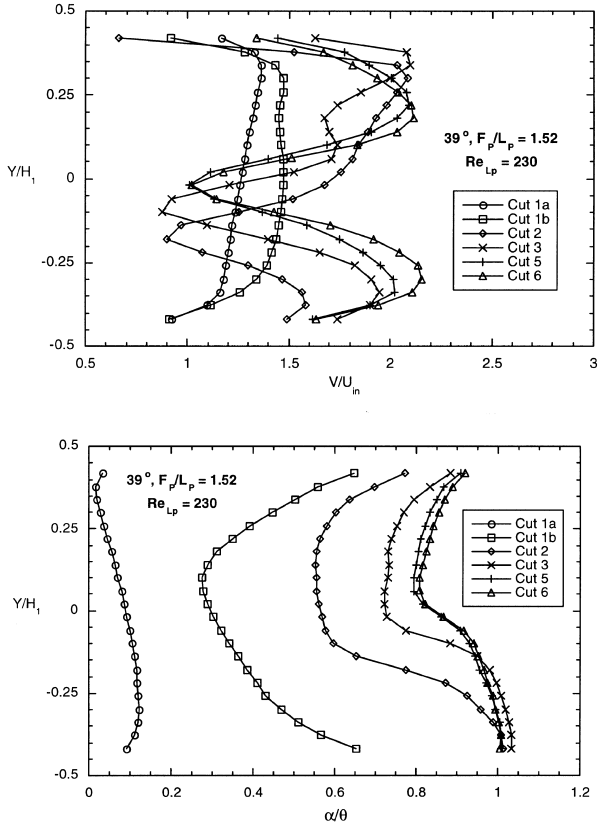

Fig. 10. (a), (b) Velocity magnitude and flow angle profiles showing development through the louver bank for $\theta = 39°$ and $F_p/L_p = 1.52$ at $Re_{Lp} = 230$.

the passage at $Y/H_1 = 0.25$, which was caused by the blockage of the next louver. The primary wake progressed from $Y/H_1 = -0.16$ at cut 2, to $Y/H_1 = -0.08$ at cut 3, and to a final position of $Y/H_1 = -0.03$ at cuts 5 and 6. This was accompanied by an increase in average flow angle from 0.40θ at cut 1b to 0.89θ at cut 5. The secondary wake was seen in the third passage at $Y/H_1 = 0.18$. By the fifth and sixth passages, the secondary wake had moved vertically until it was beyond the bulk velocity measurement range. The velocity profiles became invariant beyond the fifth louver. The development length for this fin spacing is similar to that of the $\theta = 27°$ case in that both required a development length of five louvers. The flow angle profiles showed that the flowfield was relatively constant in the fifth and sixth louver passages. The primary wake is located much lower in the passage for the 39° case relative to the 27°. This is because when the louver angle is changed for a given fin pitch the location of the louvers relative to each other change as well.

Referring back to Fig. 9, it is clear that there is not as strong a dependency on the louver angle as the fin pitch with regards to the development length. This is clear when comparing the average flow angles for the $F_p/L_p = 1.52$ case where both appear to be fully developed by the fifth louver. The one difference that does occur is that the flow angles are slightly higher for the higher louver angle.

6. Time resolved velocities downstream of the louver

As mentioned previously, time resolved velocities were measured at a position $0.5L_p$ directly downstream of the fully developed louvers for the 27° louver angle cases. A FFT routine was used to compute the energy density spectra in order to determine whether there were distinct frequencies that could be detected in the flows.

Time resolved measurements were made with $F_p/L_p = 0.76$ from a low Reynolds number to a maximum of $Re_{Lp} = 1800$, at increments of 100. Fig. 11 shows the computed energy density spectra data versus the frequency for this geometry. The data sets labeled "Inlet" were measured at the inlet to the scaled model, showing a quiet flow entered the louver bank. A distinct frequency component was evident starting at $Re_{Lp} = 1000$. The peak frequency shifted to higher values as the Reynolds number increased. These frequencies collapsed to a fairly constant Strouhal number of $St = 0.17$ for $1000 < Re_{Lp} < 1800$. The Strouhal number was based on the louver thickness, the peak frequency, and the local mean velocity. Subharmonics at twice the peak frequency were seen starting at a Reynolds number of 1100. While the peak energy level occurs over a very small range of frequencies for the lowest Reynolds number case, this range of frequencies broadens with increasing Reynolds numbers. This broadening would be expected based on the tendency for the flow to be approaching a fully turbulent condition.

Fig. 12 shows the energy density spectra for the time resolved velocity measurements in the geometry with $F_p/L_p = 0.91$. With the increase in the fin spacing, a distinct frequency component in the velocity behind the louver was seen starting at a lower Reynolds number of $Re_{Lp} = 800$. The subharmonics at twice the peak frequency, however, did not become apparent until $Re_{Lp} = 1200$ for this case. The Strouhal number for this case averaged to $St = 0.19$ for $800 < Re_{Lp} < 1800$, which were slightly higher than for the previous geometry.

Fig. 13 shows the energy density spectra for the measurements downstream of the louver with $F_p/L_p = 1.52$. This was the largest fin spacing, and frequency components began to be apparent in the flow at the smallest Reynolds number of the three cases, at $Re_{Lp} = 400$. Recall that in this geometry the wakes also traveled the farthest through the louver bank. Subharmonics at twice the primary frequency were seen at $Re_{Lp} = 700$ in this geometry. The Strouhal number was the highest at $St = 0.22$ for $400 < Re_{Lp} < 1400$, and also had the broadest range.

7. Practical significance of these results

This paper has pointed out a number of practical issues associated with the entry region of louvered fin

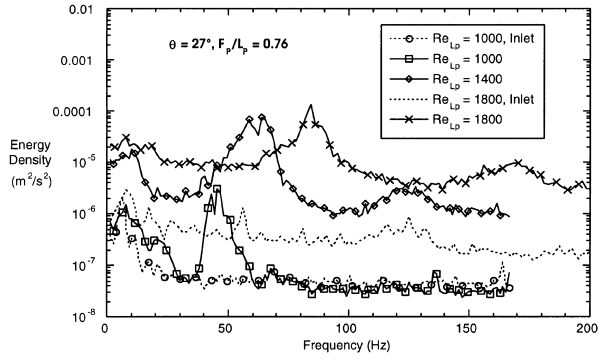

Fig. 11. Spectra of the velocity fluctuations downstream of a fully developed louver for $\theta = 27°$ and $F_p/L_p = 0.76$.

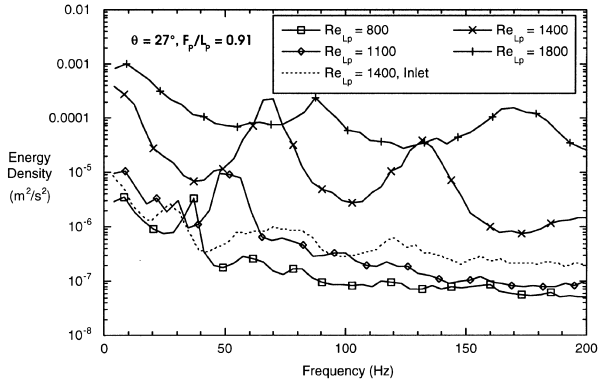

Fig. 12. Spectra of the velocity fluctuations downstream of a fully developed louver for $\theta = 27°$ and $F_p/L_p = 0.91$.

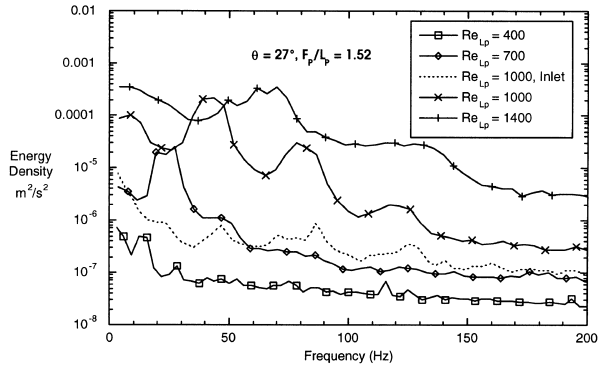

Fig. 13. Spectra of the velocity flutuation downstream of a fully developed louver for $\theta = 27°$ and $F_p/L_p = 1.52$.

heat exchangers. An understanding of this region is critical since this region can have a large impact on the overall performance of a compact heat exchanger. If one considers a compact heat exchanger where there are typically 17 streamwise louvers (as in the case we considered), a large number of those 17 louvers are in the entry region where the flow is not yet hydrodynamically fully developed. These results indicate that a significant percentage of the louvers in the streamwise array have heat transfer coefficients that vary within the heat exchanger. Most heat exchanger tests, however, are conducted through bulk testing such that results are reported by an average heat transfer coefficient. Since a large number of louvers are affected, the effect of increasing or decreasing the number of louvers in the streamwise array will have a significant impact on the overall heat transfer that takes place.

The results from this study have shown that for larger ratios of fin pitch to louver pitch the flow requires more louvers before it becomes hydrodynamically fully developed. This is of importance in designing a compact heat exchanger. As the flow becomes hydrodynamically and thermally fully developed, the average heat transfer coefficient for downstream louvers would be expected to remain fairly constant. Whether or not the average louver heat transfer coefficients increase or decrease as the flow progresses downstream in the entry region is dependent upon the Reynolds number, as pointed out by the study of DeJong and Jacobi [8]. DeJong and Jacobi showed that at low Reynolds numbers shedding vortices occurred downstream of the exit louver and as the Reynolds number increased these vortices began to occur for louvers located upstream reaching the entry region. These vortices, which could occur from the leading or trailing louver edges, were shown to significantly increase the average heat transfer along their staggered parallel plates. That increase in heat transfer occurred, however, for the condition where the upstream wake interacted directly with the downstream staggered louver. For our study, a flow periodicity was also identified through spectra. The geometries having larger ratios of fin pitch to louver pitch indicated a flow periodicity at lower Reynolds numbers than the smaller ratios of fin pitch to louver pitch. This is consistent with wakes progressing further downstream for wider fin spacings. As to whether increases in heat transfer could be expected in the entry region, this would still be dependent upon how the vortices interact with the louver.

8. Conclusions

The entry region of a louvered fin heat exchanger model is highly dependent upon the particular geometry. This study found that there was a more significant influence due to ratio of the fin pitch to louver pitch relative to the louver angle. Wake effects of upstream louvers progressed farther downstream for larger fin pitches and higher Reynolds numbers. Larger fin pitches resulted in lower average flow angles in the louver passages and longer development lengths. Higher Reynolds numbers required a longer development distance before the flow became hydrodynamically developed. When comparing the louver angle effects at the same ratio of fin pitch to louver pitch, a larger louver angle resulted in higher average flow angles and shorter development lengths.

This study showed that frequency components were observed in the flow behind the fully developed louver. These could be simply a velocity fluctuation that has been previously termed a feathery wake, or it could be the result of full scale vortex shedding. Some differences based on fin pitch were observed. First, the onset of frequency components in the developed flow downstream of the louver occurred at lower Reynolds numbers for larger fin pitches. This is consistent with the wakes progressing further downstream through the passages in the bulk flow measurements with the larger fin spacings. Second, the Strouhal number was basically constant for a fin pitch, but the value increased with increasing fin pitch.

Nomenclature

f	frequency
F_p	fin pitch
H_l	vertical distance between louvers, $F_p - t/\cos\theta$
L_p	louver pitch
Re_{Lp}	Reynolds number $= \rho U_{in} L_p/\mu$
St	Strouhal number
t	fin thickness
u	mean velocity in streamwise direction
U_{in}	mean inlet face velocity
v	mean velocity in vertical direction
V	total velocity magnitude $= (u^2 + v^2)^{1/2}$
X	streamwise coordinate direction
Y	vertical coordinate direction relative to louver, see Fig. 1(b)
α	flow angle $= \tan^{-1}(v/u)$
μ	air viscosity
θ	louver angle
ρ	air density

Acknowledgements

The authors would like to acknowledge Modine Manufacturing Company for providing the scaled-up louver models, and in particular, Drs. Steve Memory, Mark Voss, Jonathon Wattelet, and Winston Zhang for serving as contract monitors for this work.

References

[1] F.N. Beauvais, An Aerodynamic Look at Automobile Radiators, SAE Paper No. 650470, 1965.
[2] C.J. Davenport, Heat Transfer and Fluid Flow in Louvered Triangular Ducts, Ph.D. Dissertation, CNAA, Lanchester Polytechnic, 1983.
[3] C.J. Davenport, Correlations for Heat Transfer and Flow Friction Characteristics of Louvered Fin, Heat Transfer – Seattle 1983, AICHE Symposium Series, No. 225, Vol. 79, 1983, pp. 19–27.
[4] A.A. Antoniou, M.R. Heikal, T.A. Cowell, Measurements of Local Velocity and Turbulence Levels in Arrays of Louvered Plate Fins, Heat Transfer 1990, Paper No. 10-EH-18, pp. 105–110, 1990.
[5] S. Mochizuki, Y. Yagi, Characteristics of vortex shedding in plate arrays, in: W. Merzkirch (Ed.), Flow Visualization II, Washington, DC, 1982, pp. 99–103.
[6] C.H. Amon, D. Majumdar, C.V. Herman, F. Mayinger, B.B. Mikic, D.P. Sekulic, Numerical and experimental studies of self-sustained oscillatory flows in communicating channels, Int. J. Heat and Mass Transfer 35 (11) (1992) 3115–3129.
[7] L.W. Zhang, A Numerical Study of Flow and Heat Transfer in Compact Heat Exchangers, Ph.D. Dissertation, University of Illinois, Urbana, Illinois, 1996.
[8] N.C. DeJong, A.M. Jacobi, An experimental study of flow and heat transfer in parallel-plate arrays: local row-by-row and surface average behavior, Int. J. Heat and Mass Transfer 40 (6) (1997) 1365–1378.
[9] M.E. Springer, K.A. Thole, Experimental design for flowfield studies of louvered fins, Exp. Thermal Fluid Sci. 18 (3) (1998) 258–269.
[10] M.E. Springer, K.A. Thole, Flowfield Studies in Louvered Fins Relevant to Compact Heat Exchangers, University of Wisconsin, CHTL Report 98-1, 1998.
[11] R.J. Moffat, Describing the uncertainties in experimental results, Exp. Thermal Fluid Sci. 1 (1988) 3–17.